

## The Three Dimensional Extended Bridging Domain Method for Brittle Fracture

H. Talebi<sup>1</sup>, M. Silani<sup>2</sup> and T. Rabczuk<sup>1</sup>

<sup>1</sup>Institute of Structural Mechanics  
Bauhaus-University Weimar, Germany  
<sup>2</sup>Department of Mechanical Engineering  
Isfahan University of Technology, Iran

### Abstract

In this paper, a concurrent multiscale method for coupling the three dimensional continuum and molecular dynamics domain is presented. The coupling method is based on the Bridging Domain method. To handle discontinuities in continuum domain, the extended finite element method (XFEM) is used. The Lennard-Jones potential is used to model the interactions in the atomistic domain and the Cauchy-Born method is used to compute the material behaviour in the continuum domain. To show the productivity and applicability of the proposed method, two different three dimensional crack examples were modeled. The results show that the method is capable of handling dislocation nucleation and crack propagation in the three dimensional space.

**Keywords:** extended finite element method, molecular dynamics, bridging domain method, multiscale methods.

## 1 Introduction

One of the main research topics in materials science and mechanics in the last decade was to gain a fundamental understanding of material failure. Earlier approaches were based mainly on the empirical observations. Material failure depends often on the behaviour of the next lower level. Typical examples are shear bands in metallic materials, micro-cracks in quasi-brittle materials, dislocation and defects in the atomic lattice, etc. In these cases, the response of the body depends on the accuracy of the finer scale modeling.

There are different methods for modeling cracks and failure in materials both in continuum and atomistic scales. Methods which can work on the resolution of the lower scales are too expensive and hardly can be used in real engineering problems. Therefore new methods to simulate material failure are urgently needed in engineer-

ing. This was the motivation of a big class of numerical methods called multiscale methods. In these methods, different length and time scales are correlated to keep both accuracy and efficiency.

In the multiscale failure analysis of materials, different length and time scales are involved. For example, the diameter of inclusions or imperfections ('micro-voids') is between  $10^{-6}$  m to  $10^{-3}$  m, whereas the size of the structure to be examined is in the order of  $10^0$  m. Thus modeling with the resolution of the finer scale throughout the model is not currently feasible due to available computational resources. The difference in the time scales in dynamic applications is sometimes even more drastic. It was shown that the time scales at the atomic level is in the range of  $10^{-15}$  seconds while the time scale in the macro-scale level is in the order of  $10^{-4}$  seconds. Therefore, the coupling of models from different time and length scales results in some difficulties.

In the case of atomistic to continuum coupling, additional problems arise because of different assumptions in both models. For example, in the molecular dynamics, the speed of the atoms is proportional to the temperature while in continuum model, the temperature is considered as a speed independent scalar field. Without suitable coupling methods, unphysical effects such as heating or melting in the atomic system can occur.

To date, several concurrent approaches have been developed. Generally, two so-called 'Interface' coupling and 'Handshake' coupling can be distinguished. The former approach is susceptible to artificial wave reflections on the boundary (however, effective approaches to reduce artificially reflected waves have been developed recently [1]). In 'Handshake' couplings approaches, two areas from different scales are gradually transformed into each other.

One of the most popular methods in coupling MD to continuum domains is the quasi-continuum method of Tadmor et al. [2]. The coupling can be interpreted as a seamless MD to continuum transition by means of a force-field potential to a continuum potential changing. However, the nodes in the atomic field should be at the same position of the atoms which results in highly distorted FE meshes especially in the 'coarsening'. Furthermore, the propagation of defects (in MD area) requires the conversion of continuum domain to MD field.

The 'coupling of length scales' (CLS) method of Abraham et al. [3, 4] and Broughton et al. [5] links the atomic system with the continuum domain which is described by finite elements. At the transition from atomic to the continuum field, atoms are placed at the points of finite elements. By introducing a damping kernel matrix and special boundary conditions, Weinan and Huang [6] eliminated the redundant degrees of freedom on the MD boundary. A chebyshev polynomial mapping function was developed by Bayliss and Turkel [7] that can reduce artificial boundary effects.

The bridging scale method of Wagner and Liu [8] can eliminate reflection of unauthorized elastic waves on the atom/continuum transition area. In this coupling method, the continuum domain is modeled using finite elements or meshfree discretization [9]. Likewise, in the bridge area the nodes should be placed in the atom positions. The bridging method of Xia and Belytschko [10] is based on an  $L^2$  link, i.e. displacement

compatibility between atomistic and continuum field would be accomplished by means of Lagrange multipliers in weak form. In this paper, the partition of unity enriched methods and the bridging domain method (BDM) [11] are blended together for crack modeling. Here, a weak coupling between the models in the two adjacent domains is used [12, 13]. It was shown that the spurious wave reflection is minimum in this kind of coupling method [12].

It should be noted that in the XFEM-BDM coupling method, the atomistic region presents only around crack front but not along the whole length of the crack surface. This part of crack is mainly simulated by XFEM in the continuum domain. The handshake domain allows the crack to be smoothly represented from the continuum domain to atomistic domain. This advantage of XFEM-BDM coupling method over other concurrent multiscale methods such as the standard BDM or the quasi-continuum method of Tadmor et al. [2], Shenoy et al. [14] and Miller and Tadmor [15], makes this method more efficient and applicable for real physical problems. This affords the modeling and simulation of relatively long cracks, by restricting the MD model to a small zone around the crack front. Since the crack front is modeled by molecular dynamics, the creation and propagation of dislocations are easy to capture by this method.

Another advantage of the current study over the previous studies for example by Gracie and Belytschko [16] is that, this study implements a full three dimensional version which can be extended to many potentials and continuum meshes. At the many stages of the implementation, the generality of the computational and algorithmic methods were treated with care to make it usable for real physical conditions and computational sizes beyond just simple academic examples. This is achieved by coupling our in-house Extended Finite Element code to the LAMMPS molecular simulator [17] which enables usage of many great capabilities of LAMMPS. This three dimensional method enables us to study many complex phenomena which is not even observed in 2D simulations.

This paper is organized as follows. Section 2 outlines the governing equations. Crack modeling in the continuum domain using the extended finite element approach and coupling method is discussed briefly in this section. Some implementation details about coupling molecular dynamic code to finite element code are discussed in section 3. Section 4 presents two numerical examples for modeling crack problems. Finally, the conclusion of this research is presented in section 5.

## 2 Model Description and Governing Equations

### 2.1 Definitions

Consider a domain  $\Omega$  where an existing crack with the surface  $\partial\Omega_c$  is to be simulated. We define a fine scale region  $\Omega^{\text{fs}}$  modeled by molecular dynamics (MD) and place its center near the crack front. The rest of the domain is the coarse scale region  $\Omega^{\text{cs}}$

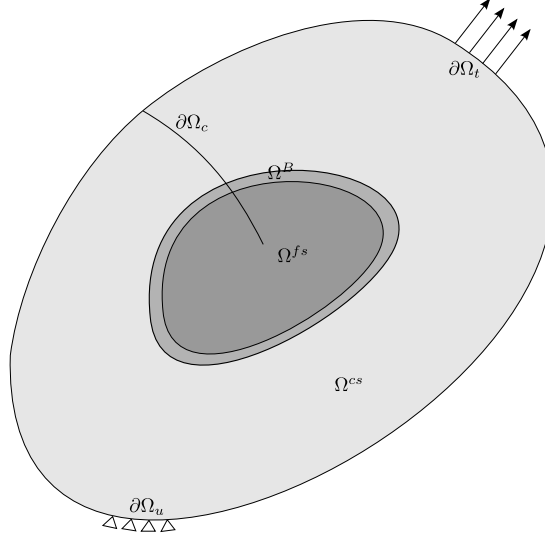


Figure 1: The relation between the fine and the coarse scale areas

where the system is described through a usual continuum formulation<sup>1</sup>. The number of atoms in sub-domain  $\Omega^{fs}$  is denoted by  $n^{fs}$ . The outer boundary of  $\Omega^{cs}$  is denoted by  $\partial\Omega^{cs}$  with  $\partial\Omega^{cs} = \partial\Omega_t^{cs} \cup \partial\Omega_u^{cs} \cup \partial\Omega_c^{cs}$  and  $\partial\Omega_t^{cs} \cap \partial\Omega_u^{cs} = \emptyset$ ,  $\partial\Omega_c^{cs} \cap \partial\Omega_u^{cs} = \emptyset$ ,  $\partial\Omega_t^{cs} \cap \partial\Omega_c^{cs} = \emptyset$ ; subscripts  $u$ ,  $t$  and  $c$  indicate 'displacement-', 'traction-' and 'crack-', respectively. Notations are summarized in Fig. 1. This molecular treatment of the crack front zone enables the description of voids, dislocations and cracks which are known to strongly influence the initiation and propagation of cracks, see, e.g. Lange [18] and Ravi-Chandar and Knauss [19].

In this study, a base crystalline material with a given lattice structure is assumed everywhere. The fine scale region  $\Omega^{fs}$  is composed of the atoms of this base lattice structure and the finite elements in this region are deactivated. This is shown in Fig. 2. In the continuum region,  $\Omega^{cs}$ , the continuum model is activated where the material behaviour is approximated by the Cauchy-Born rule, [2]. The idea of the Cauchy-Born rule is to compute the material properties and stress from the same potential used in the fine scale domain  $\Omega^{fs}$ , here the Lennard-Jones potential (LJP). In other words at every point of the continuum model, we have a very small atomistic model with the same lattice structure and force fields as the fine scale.

The sub-domain  $\Omega^{cs} \cap \Omega^{fs}$  where the continuum and atomistic descriptions cohabit is denoted by  $\Omega^B$  and is called the bridging domain, also known as the handshake, or blending domain. In the bridging domain, the continuum energy and the atomistic energy are blended through a weighting by complementary functions. One criterion which should be fulfilled is that the sum of the continuum and the atomistic energy is unchanged by the coupling method. From a kinematic point of view, in this sub-domain, the continuum model is coupled to the atomistic model by enforcing compatibility of the displacements of the atoms and that of the nodes.

<sup>1</sup>In this paper, the superscripts  $fs$  and  $cs$  denote the fine scale and coarse scale, respectively.

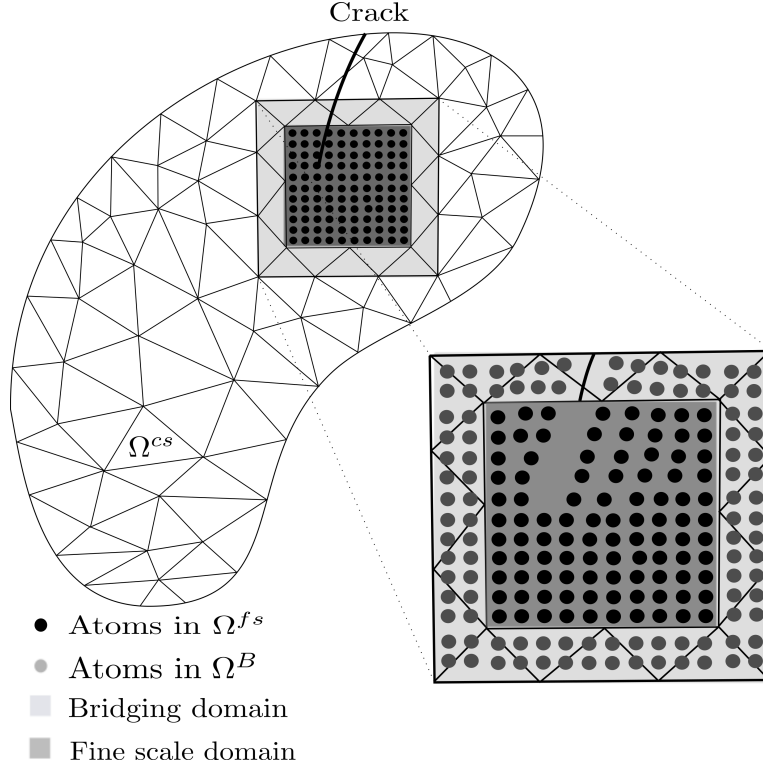


Figure 2: The solution domain including the crack and the bridging domain.

## 2.2 Fine Scale Formulation

In an isolated system, the sum of the potential and kinetic energies is constant in time. This summation is identified as the Hamiltonian and for the atomistic subdomain, it can be expressed as:

$$H^{fs}(\mathbf{x}_\alpha(t), \mathbf{p}_\alpha^{fs}(t)) = \sum_{\alpha} \frac{1}{2m_{\alpha}} \mathbf{p}_{\alpha}^{fs} \cdot \mathbf{p}_{\alpha}^{fs} + W^{fs}(\mathbf{x}_{\alpha}(t)) \quad (1)$$

where  $\mathbf{x}_{\alpha}$  and  $m_{\alpha}$  is the current position vector and mass of atom  $\alpha$  respectively. The location of atom  $\alpha$  in the reference and spacial configurations can be related by displacement vector  $\mathbf{d}$ :

$$\mathbf{x}_{\alpha} = \mathbf{X}_{\alpha} + \mathbf{d}_{\alpha} \quad (2)$$

$\mathbf{p}_{\alpha}^{fs}$  is the momentum of atom  $\alpha$  and defined by

$$\mathbf{p}_{\alpha}^{fs} = m_{\alpha} \dot{\mathbf{x}}_{\alpha} = m_{\alpha} \dot{\mathbf{d}}_{\alpha} \quad (3)$$

$W^{fs}(\mathbf{x})$  is the potential function which can be due to any kind of force fields, such as pair-wise interactions or three-body potentials:

$$W^{fs}(\mathbf{x}_\alpha) = \sum_{\alpha} W_1(\mathbf{x}_\alpha) + \sum_{\alpha, \beta > \alpha} W_2(\mathbf{x}_\alpha, \mathbf{x}_\beta) + \dots \quad (4)$$

Assuming the external potential is resulting only from a constant external force,  $\mathbf{f}_\alpha^{ext}$ , and a pair-wise potential, the total potential can be expressed as:

$$W^{fs} = -W_{fs}^{ext} + W_{fs}^{int} = - \sum_{\alpha} \mathbf{f}_\alpha^{ext} \mathbf{d}_\alpha + \sum_{\alpha, \beta > \alpha} W_{fs}(\mathbf{x}_\alpha, \mathbf{x}_\beta) \quad (5)$$

The canonical form of Hamiltonian equations in fine scale can be expressed as:

$$\begin{cases} \dot{\mathbf{p}}_\alpha^{fs} = -\frac{\partial H}{\partial \mathbf{x}_\alpha} = -\frac{\partial W^{fs}}{\partial \mathbf{x}_\alpha} \\ \dot{\mathbf{x}}_\alpha = \dot{\mathbf{d}}_\alpha = \frac{\partial H}{\partial \mathbf{p}_\alpha^{fs}} = \frac{\mathbf{p}_\alpha^{fs}}{m_\alpha} \end{cases} \quad (6)$$

Finally, these two equations can be combined to:

$$m_\alpha \ddot{\mathbf{d}}_\alpha = -\frac{\partial W^{fs}}{\partial \mathbf{x}_\alpha} = \frac{\partial W_{fs}^{ext}}{\partial \mathbf{d}_\alpha} - \frac{\partial W_{fs}^{int}}{\partial \mathbf{d}_\alpha} = \mathbf{f}_\alpha^{ext} - \mathbf{f}_\alpha^{int} \quad (7)$$

In this equation,  $\mathbf{f}_\alpha^{int}$  is internal force.

## 2.3 Coarse Scale Formulation

Let the reference and the current configurations of the domain be denoted by  $\Omega_0$  and  $\Omega$ , respectively. The material coordinates of a point in  $\Omega_0^{cs}$  are denoted by  $\mathbf{X}$  and the spatial coordinates by  $\mathbf{x}$ . The linear momentum equations are:

$$\frac{\partial P_{ji}}{\partial X_j} + \rho_0 b_i = \rho_0 \ddot{u}_i \quad (8)$$

where  $\mathbf{P}$  is the first Piola-Kirchhoff stress tensor,  $\mathbf{b}$  is the body force vector per unit mass,  $\rho_0$  is the initial density and  $\mathbf{u}$  is the displacement vector. The first Piola-Kirchhoff stress tensor can be calculated from a continuum potential:

$$\mathbf{P} = \frac{\partial w_{cs}(\mathbf{F})}{\partial \mathbf{F}} \quad (9)$$

where  $w_{cs}$  is the potential energy per unit volume and  $\mathbf{F}$  is the deformation gradient tensor. The total potential energy of the coarse model is:

$$W_{cs}^{int} = \int_{\Omega_0^{cs}} w_{cs}(\mathbf{F}) d\Omega_0^{cs} \quad (10)$$

In the coarse scale, the Hamiltonian is given by:

$$H^{cs} = K^{cs} + W^{cs} = \int_{\Omega_0^{cs}} \frac{1}{2} \rho \mathbf{v}^T \mathbf{v} d\Omega_0^{cs} + W^{cs} \quad (11)$$

$$W^{cs} = -W_{cs}^{ext} + W_{cs}^{int} = - \sum_I \mathbf{f}_I^{ext} \mathbf{u}_I + \int_{\Omega_0^{cs}} w_{cs}(\mathbf{F}) d\Omega_0^{cs} \quad (12)$$

where  $\mathbf{v}$  is the velocity vector and  $K^{cs}$  is the kinetic energy in the coarse scale. In the continuum sub-domain, the displacement field is approximated by the extended finite element method (XFEM). In this approximation, the displacement field is decomposed into a continuous part and a discontinuous part as in Belytschko and Black [20]:

$$\mathbf{u}^h(\mathbf{X}) = \underbrace{\sum_{I \in \mathcal{N}} N_I(\mathbf{X}) \mathbf{u}_I}_{\mathbf{u}^{cont}} + \underbrace{\sum_{I \in \mathcal{N}_b} N_I(\mathbf{X}) H(f_I(\mathbf{X})) \mathbf{a}_I}_{\mathbf{u}^{discont}} \quad (13)$$

where  $\mathcal{N}$  is the set of all nodes in the domain and  $\mathcal{N}_b$  is the set of nodes that belong to all elements which are completely cut by the crack. The nodal parameters  $\mathbf{u}_I$  and  $\mathbf{a}_I$  are standard and enriched degrees of freedom, respectively and  $H$  is the discontinuous enrichment (Heaviside) function:

$$H(f(\mathbf{X})) = \begin{cases} 1 & \text{if } f(\mathbf{X}) > 0 \\ 0 & \text{if } f(\mathbf{X}) < 0 \end{cases} \quad (14)$$

with

$$f(\mathbf{X}) = \text{sign}[\mathbf{n} \cdot (\mathbf{X}_I - \mathbf{X})] \min_{\mathbf{X}_I \in \partial\Omega_c} \|\mathbf{X}_I - \mathbf{X}\| \quad (15)$$

where  $\mathbf{n}$  is the outward normal to the crack surface. In this study since the crack front is modeled by the atomistic region, no crack-front enrichment is needed.

## 2.4 Coupling Method

As mentioned before, in the bridging domain method, the total energy of the system is a weighted contributions of the fine and coarse models in the bridging domain  $\Omega^B$ . To implement this concept, a scalar weight function,  $w$ , was defined which is unity outside the fine scale domain, zero inside the fine scale and smoothly varying inside the blending region:

$$w(\mathbf{X}) = \begin{cases} 1 & \forall \mathbf{X} \in \Omega^{cs} \setminus \Omega^{fs} \\ [0, 1] & \forall \mathbf{X} \in \Omega^B \\ 0 & \forall \mathbf{X} \in \Omega^{fs} \setminus \Omega^{cs}. \end{cases} \quad (16)$$

The  $w$  at any point  $\mathbf{X}$  can be computed by a normalized distance function:

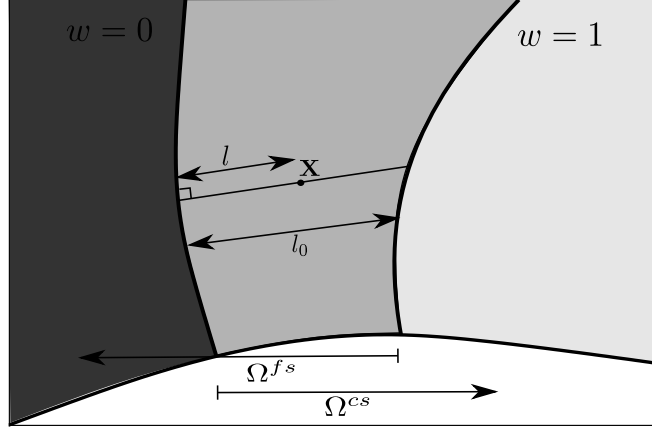


Figure 3: The weighting function in the handshake domain in two dimensions

$$w(\mathbf{X}) = \frac{l(\mathbf{X})}{l_0} \quad (17)$$

where  $l(\mathbf{X})$  is the orthogonal projection of  $\mathbf{X}$  on the interior boundary of the coarse domain  $\Omega^{cs}$  and  $l_0$  is the length of this orthogonal projection to the boundary of the fine scale  $\Omega^{fs}$ , Fig. 3.

The governing equations are derived from the Hamiltonian of the systems,  $H$ , which is the sum of the Hamiltonians of each subdomain:

$$\begin{aligned} H &= (1 - w)H^{fs} + wH^{cs} \\ &= \sum_{\alpha} (1 - w(\mathbf{X}_{\alpha})) \frac{\mathbf{p}_{\alpha}^{fs} \cdot \mathbf{p}_{\alpha}^{fs}}{2m_{\alpha}} + (1 - w)W^{fs} + \sum_I w(\mathbf{X}_I) \frac{\mathbf{p}_I^{cs} \cdot \mathbf{p}_I^{cs}}{2M_I} + wW^{cs} \end{aligned} \quad (18)$$

where  $H^{fs}$  and  $H^{cs}$  are the Hamiltonians of the fine and coarse sub-domains.  $W^{cs}$  and  $W^{fs}$  are total potential of coarse and fine scales and are defined in Eq. 12 and Eq. 5, respectively.

The Coarse and fine scale domains are constrained on the bridging domain,  $\Omega^B$  by the Lagrange multiplier method. In this overlapping domain, the fine scale displacements are required to conform coarse scale displacements. In the Lagrange multiplier method, the total Hamiltonian is written as:

$$H_L = H + \boldsymbol{\lambda}^T \mathbf{g} \quad (19)$$

where  $\boldsymbol{\lambda}$  is Lagrange multipliers vector and  $\mathbf{g}$  is the gap vector between coarse scale displacement and fine scale displacement. To compute the Lagrange multiplier unknowns we use the method described by Belytschko and Xiao [21]. Finally, we obtain the following semi-discrete equations of motion. In the following, lower case indices

indicate the coordinate directions, e.g.  $i = 1, 2, 3$  and the upper case indices indicate the finite element nodes, e.g.  $I$ .

$$\forall I \in \mathcal{N}^{\text{cs}} \forall i \in \{1, 2, 3\} : M_{IJ} \ddot{u}_{Ji} = f_{Ii}^{\text{ext}} - f_{Ii}^{\text{int}} + f_{Ii}^{\lambda \text{cs}} \quad , \quad (20)$$

$$\forall \alpha \in \llbracket 1, \dots, n^{\text{fs}} \rrbracket, \forall i \in \{1, 2, 3\} : m_{\alpha}^{\text{fs}} \ddot{d}_{\alpha i}^{\text{fs}} = f_{\alpha i}^{\text{fs}} + f_{\alpha i}^{\lambda \text{fs}} \quad , \quad (21)$$

where  $\ddot{u}_J$  and  $\ddot{d}_{\alpha}^A$  are the accelerations of node  $J$  and atom  $\alpha$ , respectively. Also, the mass matrix is computed by:

$$\forall I, J \in \mathcal{N}^{\text{cs}} : M_{IJ} = \int_{\Omega_0^{\text{cs}}} (1-w) \rho_0 N_I N_J d\Omega_0^{\text{cs}} \quad , \quad (22)$$

The mass matrix in the coarse scale is diagonalized according to the mass-lumping scheme for XFEM which was proposed by Menouillard et al. [22]. The internal forces in the coarse scale are:

$$\forall I \in \mathcal{N}^{\text{cs}}, \forall i \in \{1, 2, 3\} : f_{Ii}^{\text{int}} = \int_{\Omega_0^{\text{cs}}} (1-w) P_{ij} \frac{\partial N_I}{\partial X_j} d\Omega_0^{\text{cs}} \quad , \quad (23)$$

The forces on each atom are determined from the interatomic potential  $W$  as:

$$\forall \alpha \in \llbracket 1 \dots n^{\text{fs}} \rrbracket, \forall i \in \{1, 2, 3\} : f_{\alpha i}^{\text{fs}} = - \sum_{\beta} \frac{1}{2} (w(X_{\alpha}) + w(X_{\beta})) \frac{\partial W(r_{\alpha\beta})}{\partial d_{i\beta}^{\text{fs}}} \quad , \quad (24)$$

where  $\beta$  ranges over all atoms within the cutoff radius of atom  $\alpha$ . The forces  $f^{\lambda \text{cs}}$  in the coarse scale and  $f^{\lambda \text{fs}}$  in the fine scale, due to the coupling are given by:

$$\forall I \in \mathcal{N}^{\text{cs}}, \forall i \in \{1, 2, 3\} : f_{Ii}^{\lambda \text{cs}} = \sum_{\alpha \in \Omega_0^B} \lambda_{\alpha i} N_I(X_{\alpha}) \quad , \quad (25)$$

and

$$\forall \alpha \in \llbracket 1 \dots n^{\text{fs}} \rrbracket, \forall i \in \{1, 2, 3\} : f_{\alpha i}^{\lambda \text{fs}} = -\lambda_{\alpha i} \quad . \quad (26)$$

### 3 Some Implementation Details

The fact that continuum and atomistic (discrete) domains are coupled, creates certain difficulties in the implementation due to the different nature of the information available in both domains. For the atomistic part a code named LAMMPS [17] is adopted here. LAMMPS is a molecular dynamics code which is written in C++ and performs message-passing via MPI calls.

The LAMMPS code is coupled to an extended finite element library called PERMIX (based on Fortran 2003 standard). The coupling is done via a Fortran 2003 interface using the ISO\_C\_BINDING module. This interface allows accessing the LAMMPS object directly from the Fortran code. A new Lennard-Jones potential is implemented in LAMMPS to account for the weighting of the atoms in the bridging domain. Also, to implement the Cauchy-Born rule, a very small atomistic part is defined at the integration point level of the coarse scale which handles stress and stiffness calculation.

In this implementation we have refined Lagrange multiplier mesh to the atomistic spacing. The size of the coupling region is based on the finite element mesh and it is one element thick. To set up the problem, the following steps have been done:

1. Build the atomistic crystal with LAMMPS
2. Minimize the potential energy of the atomistic part to find the stable positions of the atoms
3. Read the finite element (coarse scale) model definitions and the coupling information from the input
4. Build the neighbour lists for the coarse scale
5. Find all the atoms in all elements i.e. the index of element which contains every atom.
6. Find the active elements, bridging elements and nodes
7. Compute the weights of the nodes and the integration points
8. Find the active atoms, bridging atoms and ghost atoms
9. Create the atomistic groups in LAMMPS based on the last step
10. Recompute atomistic and finite element nodal masses according to their weighting.
11. Set up the Lagrange multiplier points
12. Compute the coupling matrix

Similar to LAMMPS, PERMIX has similar way of domain and neighbour searches based on bin search method. This is essential for efficient attribution of nodes and elements to atoms. To find the bridging elements, Step 6, a box is defined. Then the elements which intersect with this box are located and the bridging elements are marked. To find the element containing an atom, first, the coarse scale bin that contains the atom is found. Next, all the elements in this bin are checked if they contain the atom. This check is done with computing the local coordinates of the atom according to the element. In our experience, this method is the most efficient way of locating the atoms. This method is also very general and can be used for any type of element and geometry. The computed local coordinate, is later used to compute the weighting of the atoms.

## 4 The Numerical Examples

### 4.1 Edge Crack in a Finite Plate

Consider a three dimensional single crystal with a face centered cubic (FCC) lattice which has dimensions of  $8,000 \times 800 \times 100 \text{ \AA}^3$ . In this example a straight crack of length  $620 \text{ \AA}$  is assumed present in the domain across the whole thickness. Along the left and right sides of the specimen in the continuum domain, the movement of nodes in the Y and Z direction is fixed. The continuum model consists of 197,743 hexagonal elements and 692,064 degrees of freedom. The element size is constant over the domain, about  $15 \text{ \AA}$ . An atomistic domain of size  $580 \times 365 \times 100 \text{ \AA}^3$  is placed centered around the crack front. Fig. 4 shows a schematic configuration of the system.

Since part of the crack falls within the atomistic domain, the crack must be modeled in the atomistic region as well as in the continuum region. We do not follow the generally adopted method of removing rows of atoms along the crack, as this is somewhat arbitrary and introduces extra parameters in the formulation. Instead, we modify the neighbour list of the atoms to prevent force transmission across the crack faces.

The atomistic domain is a three dimensional lattice from an FCC crystal with lattice constant  $3.645 \text{ \AA}$ . Atomic interactions are modeled by the Lennard-Jones potential with parameters  $\sigma = 2.29621 \text{ \AA}$ ,  $\epsilon = 0.467 \text{ eV}$ , and a cut-off radius of  $4.0 \text{ \AA}$ ; the mass of all atoms is taken as  $63.5 \frac{\text{gr}}{\text{mol}}$ . In this study, we have not take the temperature into account, since the focus was on the coupling of (extended) finite element method with Molecular Dynamics. However, in our development, we can easily control the temperature in the atomistic domain with Nose-Hoover thermostat method by Nose [23]. To be able to model a realistic three dimensional problem, where periodicity is usually not available, we have not used any periodic boundary in the system.

The coupling of the continuum and atomistic part is performed within a cubic box with of dimensions  $540 \times 340 \times 100 \text{ \AA}^3$ . The elements which are cut by this box are the bridging elements and the atoms which are located inside bridging elements are the bridging atoms. Consequently, the coupling region is one element wide. With this configuration the model has 1,626,240 active atoms, 166,815 bridging atoms and 148,088 ghost atoms.

The driving force for the system is introduced through a velocity boundary condition on the right and left face of the continuum region. A velocity  $0.1 \frac{\text{ \AA}}{\text{pico-seconds}}$  is set on all the nodes belonging to the right and left boundary of the continuum domain, at every time step. The time step is 0.003 pico seconds.

Fig. 5 shows the atoms with higher centro-symmetry value, at different time steps. For the current system the centro-symmetry parameter is a powerful measure of the local lattice disorder around an atom and may be used to characterize and visualize whether the atom belongs to a perfect lattice, a defect (e.g. a stacking fault or a dislocation), or a surface [24]. The centro-symmetry indicator  $CS$  is computed as explained in Kelchner et al. [25]:

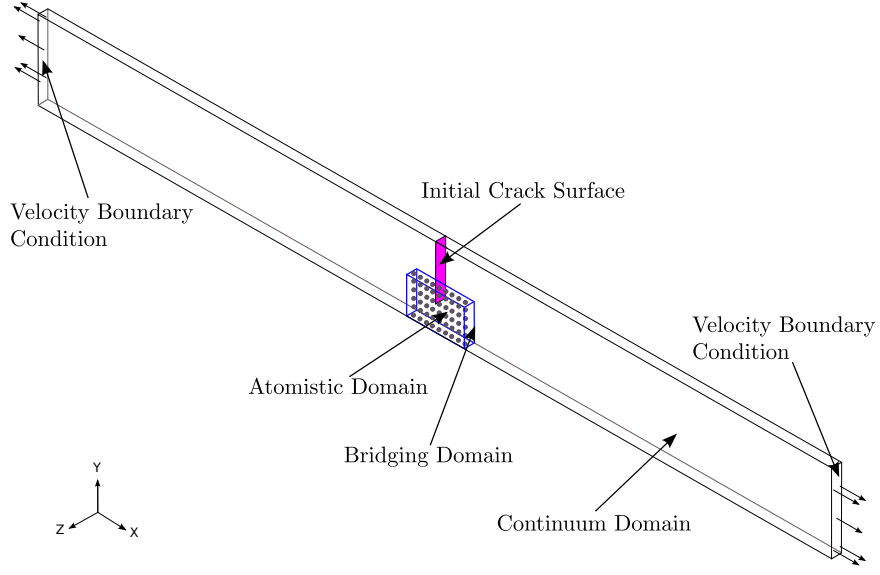


Figure 4: Schematic view of the example, bridging domain, atomistic domain and boundary conditions for an edge crack in finite plate.

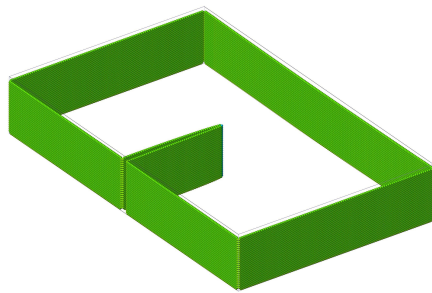
$$CS = \sum_{i=1}^{\frac{N}{2}} \left| \mathbf{R}_i + \mathbf{R}_{i+\frac{N}{2}} \right|^2, \quad (27)$$

where  $N$  is the number of nearest neighbours for each atom in the underlying lattice of atoms. For example here  $N = 12$  for the FCC lattice.  $\mathbf{R}_i$  and  $\mathbf{R}_{i+\frac{N}{2}}$  are vectors from the atom of interest to a particular pair of nearest neighbours. The value in the sum is computed for each atom, and the  $N/2$  smallest quantities are used. For an atom on a lattice site, surrounded by atoms on a perfect lattice, the centro-symmetry parameter will be 0. It will be also near 0 for small thermal perturbations of a perfect lattice.

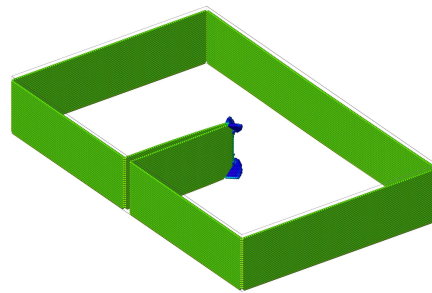
Fig. 6 shows the stress contours at four different time steps which are the same time steps as in Fig. 5. The atomistic stress computed here is the virial stress tensor. The symmetric virial stress tensor for pair potentials such as the one used here is defined in Robert [26] and Subramaniyan and Sun [27]:

$$\sigma_{ij}^V = \frac{1}{V} \sum_{\alpha} \left[ \frac{1}{2} \sum_{\beta=1}^N \left( R_i^{\beta} - R_i^{\alpha} \right) F_j^{\alpha\beta} - m^{\alpha} v_i^{\alpha} v_j^{\alpha} \right] \quad (28)$$

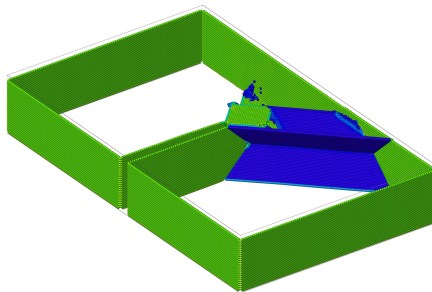
where  $(i, j)$  range over the spatial directions,  $x, y, z$ .  $\beta \in \llbracket 1, \dots, N \rrbracket$  ranges over the  $N$  neighbors of atom  $\alpha$ ,  $R_i^{\alpha}$  is the coordinate of atom  $\alpha$  in the  $i$  direction,  $F_j^{\alpha\beta}$  is the force on atom  $\alpha$  from atom  $\beta$  along the  $j$  direction,  $V$  is the total volume,  $m^{\alpha}$  is the mass of atom  $\alpha$  and  $v^{\alpha}$  is the velocity of atom  $\alpha$ . The definition of virial stress involves the instantaneous velocities only due to thermal fluctuations. Note that to obtain the equivalent continuum Cauchy stress, the virial stress from the molecular



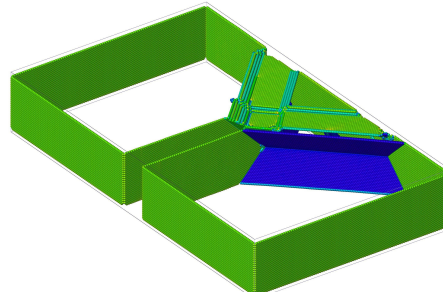
(a)



(b)



(c)



(d)

Figure 5: The propagation of the crack front and dislocations shown with atoms with high centro-symmetry value in different time steps (a) step 32,400, (b) step 33,800, (c) step 49,800, (d) step 63,400.

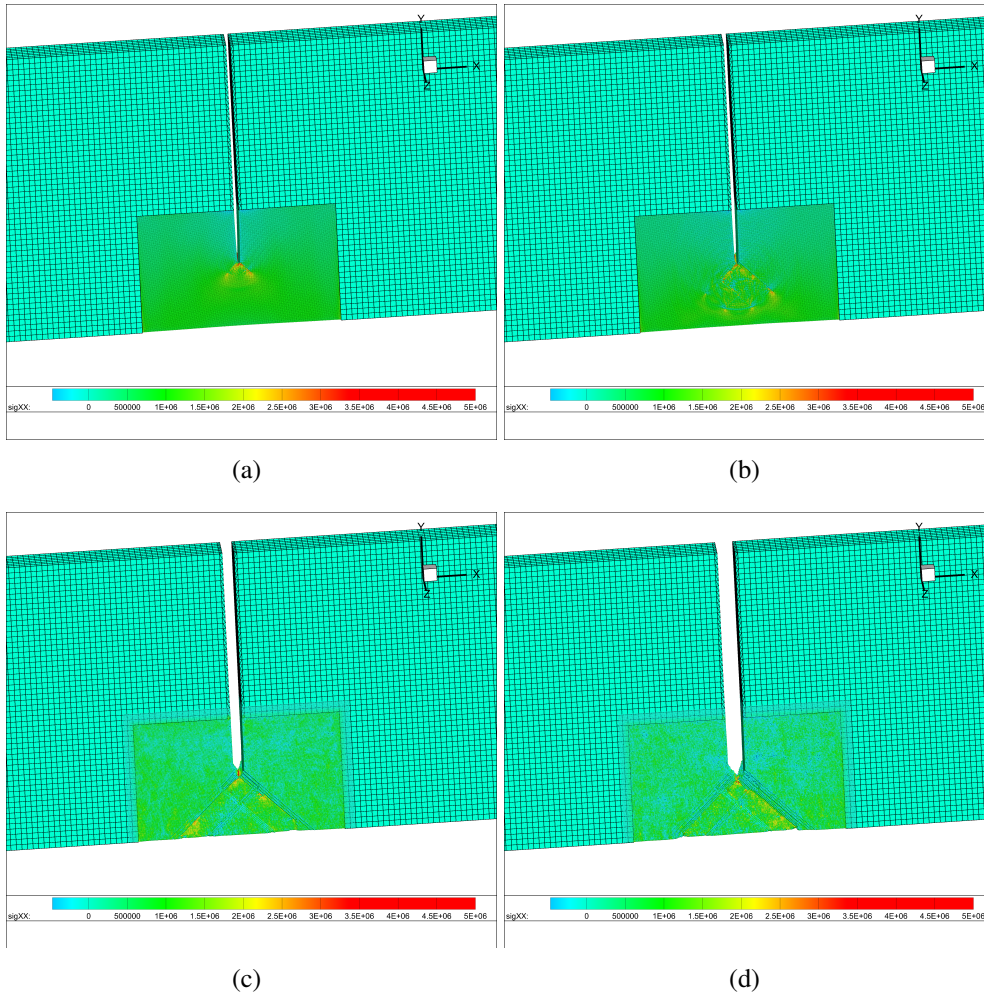


Figure 6: The stress contour of the specimen in different time steps (a) step 32,400, (b) step 33,800, (c) step 49,800, (d) step 63,400.

dynamics (MD) simulations has to be averaged over time and space, as explained in Buehler [28].

In Fig. 6(a) and (b) a stress concentration is visible, that is initially confined at the crack front; subsequently when propagation occurs, the stress waves are emitted from the crack tip. From Fig. 6(c) and (d) the surface effects of the third dimension are also evident. From this figure we also notice the stress distribution around the dislocations and the crack. Such complex mechanisms of crack and dislocations could not be predicted by any classical continuum description of motion.

## 4.2 Double-Edge-Cracked Specimen Under Combination of Shear and Tension

In this example, a double-edge-cracked specimen was considered. Here, we have two cracks under combination of shear and tension loading. Fig. 7 shows the geometry of the example, location of the cracks and boundary conditions. For modeling continuum domain, 55778 elements and 254016 degrees of freedom were used. The dimensions of the specimen were  $2,000 \times 2,000 \times 20 \text{ \AA}^3$ . For the atomistic domain, a cubic cell of  $1,100 \times 1,100 \times 20 \text{ \AA}^3$  was considered in the middle of the continuum domain. Two  $750 \text{ \AA}$  length edge cracks were put in the middle of both lateral sides of the domain. The atomistic domain covers both crack tips. The specimen was fixed at the bottom surface and a combination of shear and tension velocity boundary conditions were applied at the top surface, Fig. 7. The velocities in x and y directions were 0.1 and  $0.1 \frac{\text{\AA}}{\text{pico-seconds}}$  respectively. The material parameters were considered the same as the previous example.

The coupling of the continuum and atomistic part is performed within a cubic box with of dimensions  $1050 \times 1050 \times 20 \text{ \AA}^3$ . Same as the previous example, the coupling region is one element wide. Finally, the model has 2,094,840 active atoms, 93,804 bridging atoms and 72,366 ghost atoms.

Fig. 8 shows the history of the virial stress in the atomistic domain. Fig. 8 (a) shows the time of dislocation nucleation. Fig. 8 (b) and (c) show the propagation of dislocation and crack nucleation respectively. Fig. 8 (d) represent the crack propagation direction. Fig. 9 shows the same stress history for whole specimen. Here, the shear stress was plotted instead.

## 5 Conclusion

We presented a coupling method for bridging a three dimensional extended finite element treatment of cracks and molecular dynamics. This method is based on an overlapping domain-decomposition scheme where the displacement compatibility conditions in the overlapping sub-domain are enforced by Lagrange multipliers. We showed how the method can be successfully used to simulate the propagation of a cracks and dislocations, where an atomistic domain is placed on top of the three dimensional

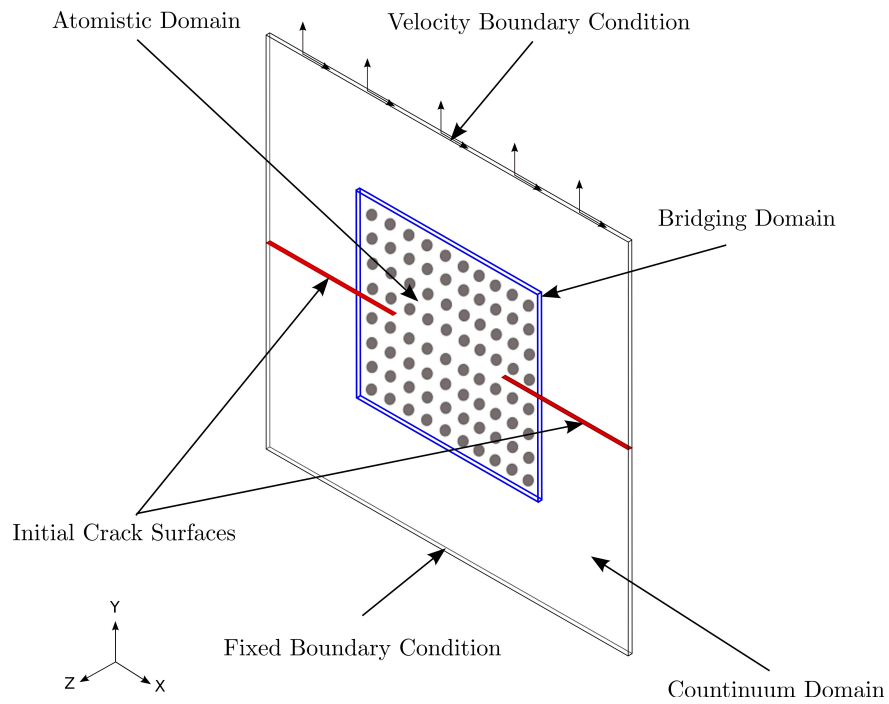


Figure 7: Schematic representation of the double-edge-notched specimen under combined loading, including bridging domain, atomistic domain and boundary conditions.

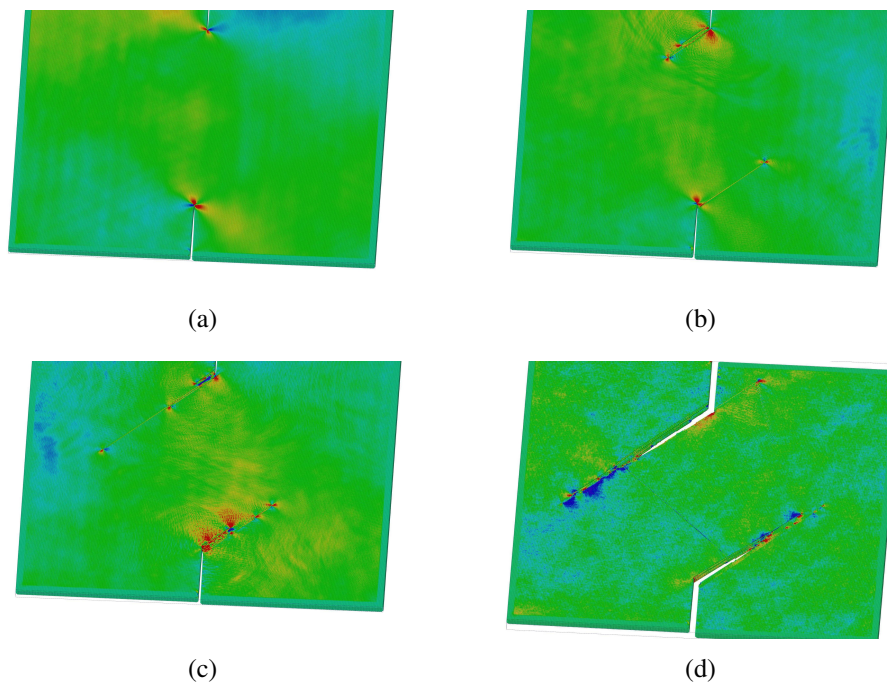


Figure 8: The virial stress contours of the atomistic domain in different time steps (a) step 25,800, (b) step 31,800, (c) step 35,800, (d) step 77,200.

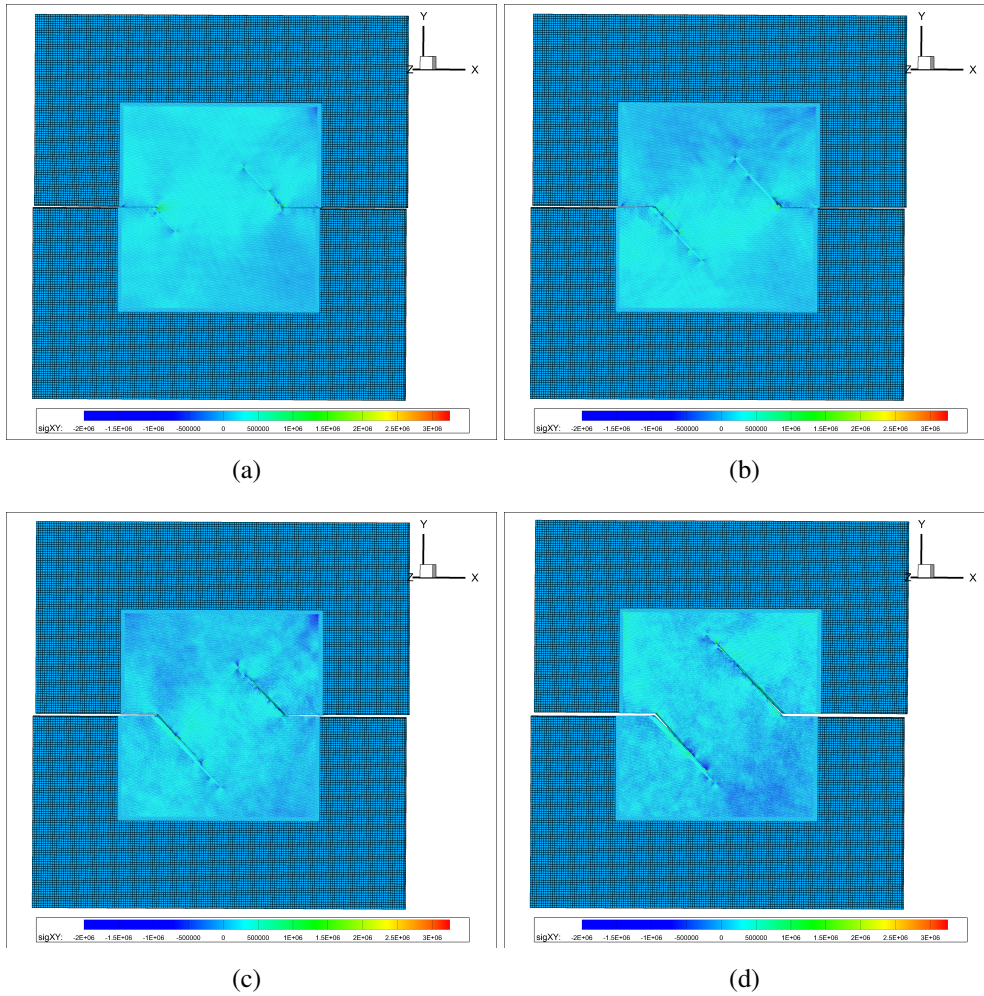


Figure 9: The stress contours of of the specimen in different time steps (a) step 25,800, (b) step 29,600, (c) step 43,800, (d) step 64,800.

extended finite element domain, around the crack front. We also computed the centrosymmetry parameter and the virial stress tensor in the atomistic region. We have observed that our three dimensional coupled method is capable of representing the crack and dislocation propagation for much fewer degrees of freedom than a direct numerical simulation.

## References

- [1] E. Saether, V. Yamakov, and EH Glaessgen. An embedded statistical method for coupling molecular dynamics and finite element analyses. *International Journal for Numerical Methods in Engineering*, 78(11):1292–1319, 2009.
- [2] E.B. Tadmor, M. Ortiz, and R. Phillips. Quasicontinuum analysis of defects in solids. *Philosophical Magazine A*, 73(6):1529–1563, 1996.
- [3] F.F. Abraham, J.Q. Broughton, N. Bernstein, and E. Kaxiras. Spanning the length scales in dynamic simulation. *Computational Physics*, 12:538–546, 1998.
- [4] F.F. Abraham, J.Q. Broughton, N. Bernstein, and E. Kaxiras. Spanning the continuum to quantum length scales in a dynamic simulation of brittle fracture. *Europhy. Lett.*, 44:783–787, 1998.
- [5] J.Q. Broughton, F.F. Abraham, N. Bernstein, and E. Kaxiras. Concurrent coupling of length scales: Methodology and application. *Physical Review B*, 60: 2391–2403, 1999.
- [6] E. Weinan and Z.Y. Huang. A dynamic atomistic-continuum method for the simulations using a bridging scale decomposition. *Journal of Computational Physics*, 182:234–261, 2002.
- [7] A. Bayliss and E. Turkel. Mappings and accuracy for chebychev pseudospectral approximations. *Journal of Computational Physics*, 101:349–359, 1992.
- [8] G. Wagner and W.K. Liu. Coupling of atomistic and continuum simulations using a bridging scale decomposition. *Journal of Computational Physics*, 190: 249–274, 2003.
- [9] Hossein Talebi, Cristbal Samaniego, Esteban Samaniego, and Timon Rabczuk. On the numerical stability and mass-lumping schemes for explicit enriched meshfree methods. *International Journal for Numerical Methods in Engineering*, 2011. ISSN 1097-0207. doi: \$10.1002/nme.3275\$. URL <http://dx.doi.org/10.1002/nme.3275>.
- [10] S.P. Xiao and T. Belytschko. A bridging domain method for coupling continua with molecular dynamics. *Computer Methods in Applied Mechanics and Engineering*, 193:1645–1669, 2004.
- [11] H.B. Dhia and G. Rateau. The arlequin method as a flexible engineering design tool. *International Journal for Numerical Methods in Engineering*, 62:1442–1462, 2005.
- [12] T. Belytschko M. Xu. Conservation properties of the bridging domain method for coupled molecular/continuum dynamics. *International Journal for Numerical Methods in Engineering*, 76:278–294, 2008.

- [13] R. Gracie and T. Belytschko. Concurrently coupled atomistic and XFEM models for dislocations and cracks. *International Journal for Numerical Methods in Engineering*, 78(3):354–378, 2009.
- [14] V.B. Shenoy, R. Miller, E.B. Tadmor, D. Rodney, R. Phillips, and M. Ortiz. An adaptive finite element approach to atomic-scale mechanics-the quasicontinuum method. *Arxiv preprint cond-mat/9710027*, 1997.
- [15] R.E. Miller and E.B. Tadmor. The quasicontinuum method: Overview, applications and current directions. *Journal of Computer-Aided Materials Design*, 9(3): 203–239, 2002.
- [16] R. Gracie and T. Belytschko. An adaptive concurrent multiscale method for the dynamic simulation of dislocations. *International Journal for Numerical Methods in Engineering*, 2011.
- [17] S. Plimpton. Fast parallel algorithms for short-range molecular dynamics. *Journal of Computational Physics*, 117(1):1–19, 1995.
- [18] F.F. Lange. The interaction of a crack front with a second-phase dispersion. *Philosophical Magazine*, 22(179):983–992, 1970.
- [19] K. Ravi-Chandar and W.G. Knauss. An experimental investigation into dynamic fracture: II. microstructural aspects. *International Journal of Fracture*, 26(1): 65–80, 1984.
- [20] T. Belytschko and T. Black. Elastic crack growth in finite elements with minimal remeshing. *International Journal for Numerical Methods in Engineering*, 45(5): 601–620, 1999.
- [21] T. Belytschko and S.P. Xiao. Coupling methods for continuum model with molecular model. *International Journal for Multiscale Computational Engineering*, 1:115–126, 2003.
- [22] T. Menouillard, J. Réthoré, A. Combescure, and H. Bung. Efficient explicit time stepping for the eXtended Finite Element Method (X-FEM). *International Journal for Numerical Methods in Engineering*, 68(9):911–939, 2006.
- [23] S. Nose. Constant-temperature molecular dynamics. *Journal of Physics: Condensed Matter*, 2:115–119, 1990.
- [24] C. Mi, D.A. Buttry, P. Sharma, and D.A. Kouris. Atomistic insights into dislocation-based mechanisms of void growth and coalescence. *Journal of Mechanics Physics of Solids*, 59:1858–1871, 2011.
- [25] C.L. Kelchner, S.J. Plimpton, and J.C. Hamilton. Dislocation nucleation and defect structure during surface indentation. *Physical Review B*, 58(17):11085, 1998.
- [26] J.S. Robert. Comments on virial theorems for bounded systems. *American Journal of Physics*, 51:940–942, 1983.
- [27] A.K. Subramaniyan and C.T. Sun. Continuum interpretation of virial stress in molecular simulations. *International Journal of Solids and Structures*, 45(14–15):4340–4346, 2008.
- [28] M.J. Buehler. *Atomistic modeling of materials failure*. Springer Verlag, 2008.